



Contents lists available at ScienceDirect

Catalysis Communications

journal homepage: www.elsevier.com/locate/catcom



BiOX (X = Cl, Br, I) photocatalysts prepared using NaBiO₃ as the Bi source: Characterization and catalytic performance

Xiaofeng Chang^{a,b}, Jun Huang^a, Cheng Cheng^c, Qian Sui^a, Wei Sha^d, Guangbin Ji^b, Shubo Deng^a, Gang Yu^{a,*}

^a POPs Research Center, Department of Environmental Science and Engineering, Tsinghua University, Beijing 100084, PR China

^b Nanomaterials Research Institute, College of Materials Science and Technology, Nanjing University of Aeronautics and Astronautics, Nanjing 210016, PR China

^c Department of Materials, Loughborough University, Loughborough, Leicestershire LE11 3TU, United Kingdom

^d Department of Electrical and Electronic Engineering, University of Hong Kong, Pokfulam Road, Hong Kong

ARTICLE INFO

Article history:

Received 31 July 2009

Received in revised form 20 November 2009

Accepted 25 November 2009

Available online xxxxx

Keywords:

Photocatalysis

Bismuth oxyhalides

NaBiO₃

Endocrine disrupting chemicals

ABSTRACT

The Bismuth oxyhalides, crystalline BiOX (X = Cl, Br, I) were prepared via a facile method, using NaBiO₃ and HX aqueous solutions as the raw materials for the first time. The systematic microstructure and optical property characterizations of the BiOX photocatalysts demonstrated the reliability of this new and facile preparation approach. The photocatalytic activity on the degradation of typical phenolic endocrine disrupting chemicals over BiOX and P25 were evaluated under Xenon-light irradiation and the initial photocatalytic mechanism was discussed based on the band edge potential analysis.

© 2009 Published by Elsevier B.V.

To date, titania has been employed in photocatalytic method to decompose many organic pollutants under ultraviolet light irradiation, due to its various advantages of low cost, high photocatalytic activity, chemical stability and non-toxicity, etc. [1]. However, the photocatalytic activity of titania in visible light is very low due to its wide band gap (3.0–3.2 eV), which prevents the efficient absorption of sunlight. Recently, the development of visible light sensitive photocatalysts has received considerable attentions as an alternative for the treatment of wastewater.

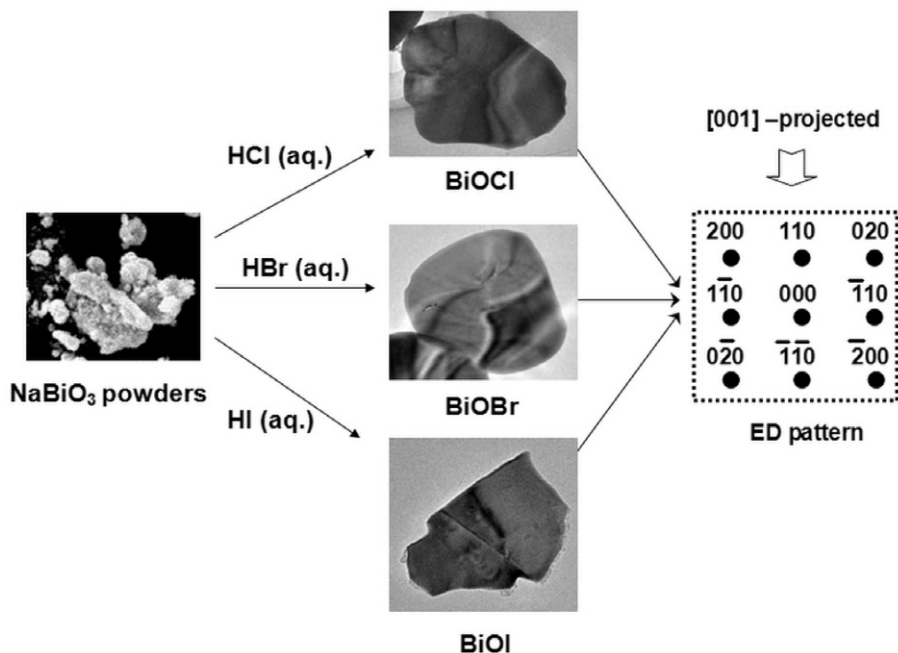
Bismuth oxyhalides (BiOX (X = Cl, Br, I)) semiconductors have demonstrated excellent photocatalytic activities and are offering a new family of promising photocatalysts [2–7]. In this study, we developed a new route for the preparation of BiOX photocatalysts, using NaBiO₃ and HX (X = Cl, Br, I) aqueous solutions as the raw materials. The microstructure of the photocatalysts was characterized and their photocatalytic activities on the degradation of four kinds of typical phenolic endocrine disrupting chemicals (EDCs) under Xenon-light irradiation were evaluated and discussed.

Scheme 1 illustrates the synthesis of single-crystalline BiOX, which owns the same [0 0 1] direction (demonstrated by Selected Area Electron Diffraction pattern, SAED). X-ray Diffraction (XRD) measurement was used to investigate the phase structures of the as-prepared samples. The patterns of BiOX samples are shown in Fig. 1. All of the detectable peaks in pattern a, b and c can be as-

signed to the tetragonal phase of BiOCl (JCPDS Card No. 82-0485), BiOBr (JCPDS Card No. 78-0348) and BiOI (JCPDS Card No. 73-2062), indicating a high purity of the products. The narrow broadening of the peaks implies well-crystallized Bismuth oxyhalides materials. X-ray Photoelectron Spectroscopy (XPS) characterization was employed to further confirm the purity of the BiOX samples. It can be observed that the spin orbit splitting peaks of Bi 4f level is split into two peaks, which are assigned to the Bi 4f_{5/2}, Bi 4f_{7/2}, respectively. The peaks were centered at 165.1 and 159.8 eV in the BiOX samples corresponding to the binding energy of Bi 4f_{5/2} and Bi 4f_{7/2}, demonstrating that the main chemical states of Bismuth element in the samples were tri-valence [8]. The results from the XPS and XRD demonstrate that there were unreduced Bi₂O₅ (V) phases in the samples.

The sheet-morphology of BiOCl, BiOBr and BiOI samples was observed on Field Emission Gun-Scanning Electronic Microscope (FEG-SEM). Meanwhile, the Energy Dispersive X-ray analysis (EDX) results indicated that Bi, O and X element from the crystals were in stoichiometric amount. The Bright-Field Transmittance Electronic Microscopy (BF-TEM) images of BiOX series crystals were recorded by using a small objective aperture that selected only the (0 0 0) central transmitted beam, showing that the particle sizes of BiOX were around 690 nm, 650 nm and 120 nm, respectively. Such results were in accordance with the FEG-SEM results. The particles were found to have single crystalline feature of the BiOX samples, shown by electron diffraction patterns and additionally proved by high-resolution lattice imaging of individual

* Corresponding author. Tel.: +86 10 6278 7137; fax: +86 10 6279 4006.
E-mail address: yg-den@tsinghua.edu.cn (G. Yu).



Scheme 1. Illustration of the synthesis of sheet-shaped single-crystalline BiOX, which own the same [0 0 1] direction.

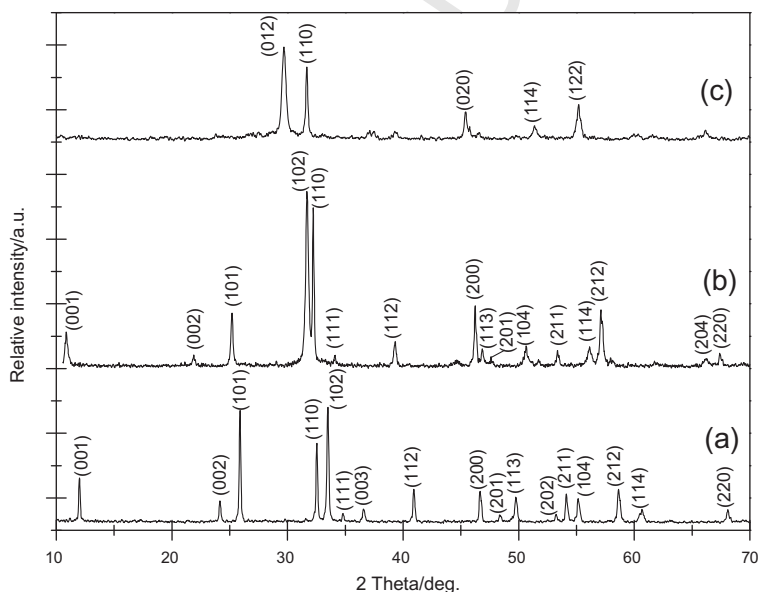


Fig. 1. XRD patterns of BiOCl (a), BiOBr (b) and BiOI (c).

84 particles. The dark field (DF) TEM images, recorded using a smaller
85 objective aperture with the selected reflections of $\{1\bar{1}0\}$, $\{1\bar{1}0\}$
86 and $\{200\}$, showed the existence of strains in each particle of BiO-
87 Cl, BiOBr and BiOI, respectively. The strains might be attributed to
88 the deformation during the synthetic process. If a particle is single
89 crystalline and has no strain, its DF-TEM photograph will be uni-
90 form in contrast. Otherwise if an image shows DF variation in con-
91 trast, the particle is likely to have strains, owing to the fact that the
92 strain has effects on the diffraction behaviors of the electrons,
93 resulting in dramatic contrast change. The high resolution TEM
94 images of BiOX crystals also showed the interplanar spacing was
95 0.275 nm, corresponding to the $\{110\}$ planes of tetragonal system
96 of BiOX crystals. The result further confirms that the BiOX sheets
97 are perpendicular to the c axis with $[001]$ direction.

The microstructure analysis mentioned above demonstrates
that the crystalline BiOX can be formed using NaBiO₃ and HX aqueous
solutions as starting materials. The valence state changes of Bi
element in NaBiO₃ and BiOX suggest that the oxidation–reduction
reaction took place during the preparation process. NaBiO₃ was
used as a selective oxidizing agent, which cleaved glycols [9].
Although the standard reduction potential of Bi (V)/Bi (III) is un-
known by now, our study shows that NaBiO₃ can oxidize HX
molecular to form Bi³⁺ and X₂ products. The BiOX products can
be formed when Bi³⁺ reacted with X⁻ in H₂O media, due to the
low solubility product constant (K_{sp}) of BiOX. In fact, some irritat-
ing gases can be found when preparing BiOCl and BiOBr photocat-
alysts, and the violet gas also can be seen when drying the BiOI
photocatalyst which was not washed thoroughly by water and eth-

anol. On the basis of the discussion above, the reaction that occurred in the formation of the BiOX crystal may be illustrated as follows:

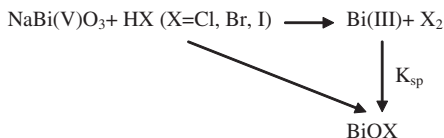


Fig. 2(a) shows the UV-Vis diffuse reflectance spectra (UV-Vis DRS) of BiOX photocatalysts. It could be found that the optical absorptions of the photocatalysts started at about 374, 434 and 682 nm, corresponding to the absorption edge of BiOCl, BiOBr and BiOI, respectively. The band gaps are also determined with the following equation,

$$\alpha \cdot E_{\text{photon}} = K \cdot (E_{\text{photon}} - E_g)^n \quad (1)$$

where α is the absorption photon coefficient, E_{photon} is the discrete photo energy, K is a constant, and E_g is the band gap energy, n depends on the type of optical transition in the gap region [10]. According to the reference [11], both of the values n for BiOX were determined to be 2, and the results were in agreement with that of previous studies [2,7]. A classical Tauc's approach is employed to evaluate the band gap of the samples, as given in Fig. 2(b). The extrapolated value (the straight lines to the x axis) of E at $x = 0$ determined the adsorption edge energies corresponding to $E_g = 1.76, 2.75$ and 3.19 eV, for BiOI, BiOBr and BiOCl, respectively. Meanwhile, the Commission International de L'Eclairage (CIE) coordinates (displayed in Fig. 2(c)) of BiOCl, BiOBr and BiOI were calculated as follows,

$$x = \frac{\int_{380}^{780} A(\lambda) \cdot x_1(\lambda) d\lambda}{\int_{380}^{780} A(\lambda) \cdot [x_1(\lambda) + y_1(\lambda) + z_1(\lambda)] d\lambda} \quad (2)$$

$$y = \frac{\int_{380}^{780} A(\lambda) \cdot y_1(\lambda) d\lambda}{\int_{380}^{780} A(\lambda) \cdot [x_1(\lambda) + y_1(\lambda) + z_1(\lambda)] d\lambda} \quad (3)$$

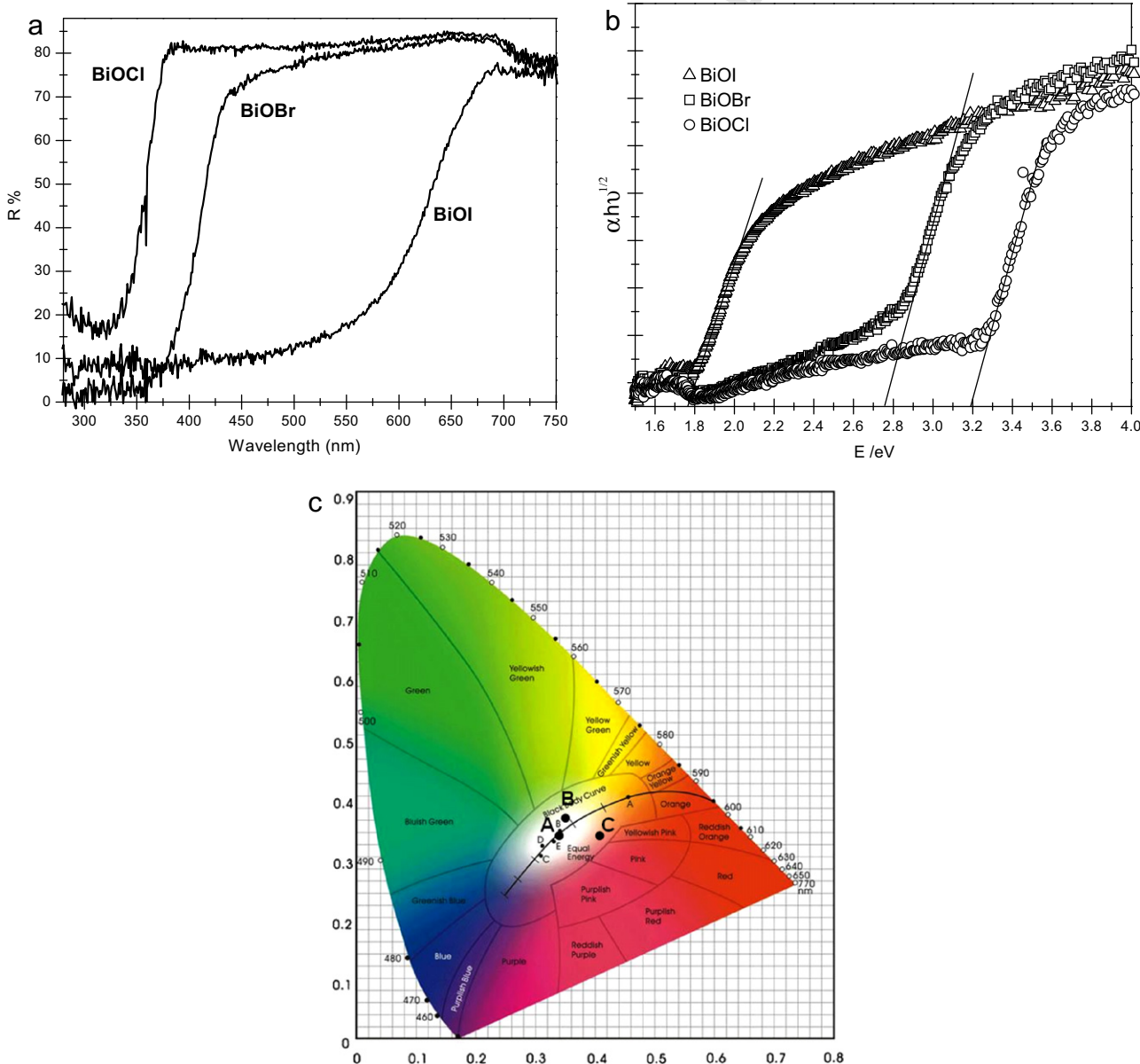


Fig. 2. (a) UV-Vis DRS spectra of BiOX photocatalysts. (b) Plots of $\alpha h\nu^{1/2}$ vs photon energy (E) for BiOX photocatalysts. (c) CIE coordinates of BiOCl (Point A), BiOBr (Point B) and BiOI (Point C) semiconductors.

where x, y is the CIE coordinates, $A(\lambda)$ is the transmittance with different wavelengths, $x1(\lambda)$, $y1(\lambda)$ and $z1(\lambda)$ is the color rendering index with different wavelength in XYZ color space. The CIE coordinates of BiOCl, BiOBr and BiOI were calculated at (0.3383, 0.3354), (0.3528, 0.3559) and (0.4075, 0.3436), respectively. The CIE results also demonstrate the visible-light-absorption characteristic of BiOBr and BiOI crystals.

4-Nonylphenol (4-NP), 4-*t*-octylphenol (4-*t*-OP), sodium pentachlorophenate (PCP-Na) and bisphenol A (BPA) are typical phenolic EDCs, which have been received great concerns worldwide due to their endocrine disrupting effect [12,13]. Our previous studies demonstrated that PCP-Na [14] and 4-*t*-OP [15] in aqueous solutions can be efficiently decomposed on NaBiO₃ photocatalyst under visible light irradiation. In our photocatalytic evaluations, the photocatalytic activities of BiOX towards them were studied. It is found that the behaviors of both photolysis and adsorption of the photocatalysts were very weak (<6%). Initial photocatalytic kinetics indicates that the photocatalytic degradation of PCP-Na over BiOX was apparently in accordance with first-order kinetics of the Langmuir–Hinshelwood model (as given in Fig. 3(a)), demonstrating the nature of the catalysis. The apparent rate constant (k) was determined to be 0.00106 min⁻¹, 0.00789 min⁻¹ and 0.03805 min⁻¹ for BiOCl, BiOBr and BiOI, respectively. And under Xenon-lamp light irradiation, after 1 h reaction, the degradation efficiency of PCP-Na over BiOCl, BiOBr and BiOI was 95.9%, 35.2% and 8.9%, respectively.

As shown in Fig. 3(b), it also can be seen that BiOI had the best photocatalytic efficiency to remove these four kinds of phenolic EDCs from aqueous solution within 1 h. UV spectra of 4-NP, 4-*t*-OP and BPA also indicated the intensities of their absorption peaks of conjugated structures were decreased along the photocatalytic process. The High Performance Liquid Chromatography (HPLC) results also suggested the destruction of the conjugated structures led to the formation of some new molecules in the aqueous solution because some weak chromatographic signals with different retention times could be observed after the photocatalysis. This indicates the formation of some long-lived by-products, which had low reaction rates with hydroxyl radicals or holes.

The conduction band (CB) edge of BiOX semiconductors at the point of zero charge was calculated by the equation as follows [16]:

$$E_{CB} = X - E^c - 1/2E_g \quad (4)$$

where X is the absolute electronegativity of the semiconductor; E^c is the energy of free electrons on hydrogen scale (≈ 4.5 eV) and E_g is

the band gap of the semiconductor. The schematic band structure of BiOX and TiO₂ photocatalysts shows that the band gap of BiOBr or BiOI was smaller than that of the traditional TiO₂ photocatalyst, suggesting their potential photocatalytic activity under visible light irradiation. On the other hand, it is also found that all of the valence band (VB) edge potentials of BiOX photocatalysts were more positive than the oxidation potential of H₂O₂ (1.77 eV) and O₃ (2.07 eV), indicating that such photocatalysts may have much stronger oxidation abilities [4].

It is noted that the potentials of conduction bands in BiOX are not sufficient to reduce oxygen due to the fact that the potentials for single-electron reduction of oxygen have higher negativity than 0 V vs SHE. Thus the photo-generated holes in BiOX semiconductors may play a significant role during the photocatalytic process. Compared to BiOCl and BiOBr photocatalysts, BiOI can absorb more photons to achieve the electron-excited process. More hydroxyl radicals or holes may be produced under the Xenon-light irradiation, and thus the highest photocatalytic activity could be obtained.

Driven by the light from Xenon lamp, the photocatalytic activity of the BiOCl was the lowest among the series of BiOX photocatalysts because of its wide band gap. Meanwhile, it is very interesting to find that the BiOCl showed better photocatalytic activity, compared to the nano-sized TiO₂ (P25), although their band gap values were similar. The result might be due to the calculated VB potential of BiOCl (~ 3.45 eV), more positive than that of TiO₂ (~ 3.1 eV), suggesting its stronger oxidative ability. In addition, the layered structure of BiOCl can polarize the related atoms and orbitals by supporting large enough space [2,17], resulting in an increase in the electron-hole separation efficiency through the appeared dipole, and thus the enhanced photocatalytic activity was observed. On the basis of the results and discussions above, the existence of the photocatalytic process was proved, however, detailed mechanism is still under investigation.

In summary, this short communication reports a facile method to the preparation of single-crystalline BiOX photocatalysts, using NaBiO₃ and HX aqueous solutions as the raw materials. The XRD and XPS characterizations confirmed the formation and purity of the BiOX photocatalysts. The TEM and SAED analysis showed the fine crystalline feature of the BiOX. The band gaps of BiOCl, BiOBr and BiOI were estimated at 3.19, 2.75 and 1.76 eV, respectively. The band edge calculation of BiOX semiconductors at the point of zero charge suggests that the conduction bands in BiOX are not sufficient to reduce oxygen. The photocatalytic activity evaluation

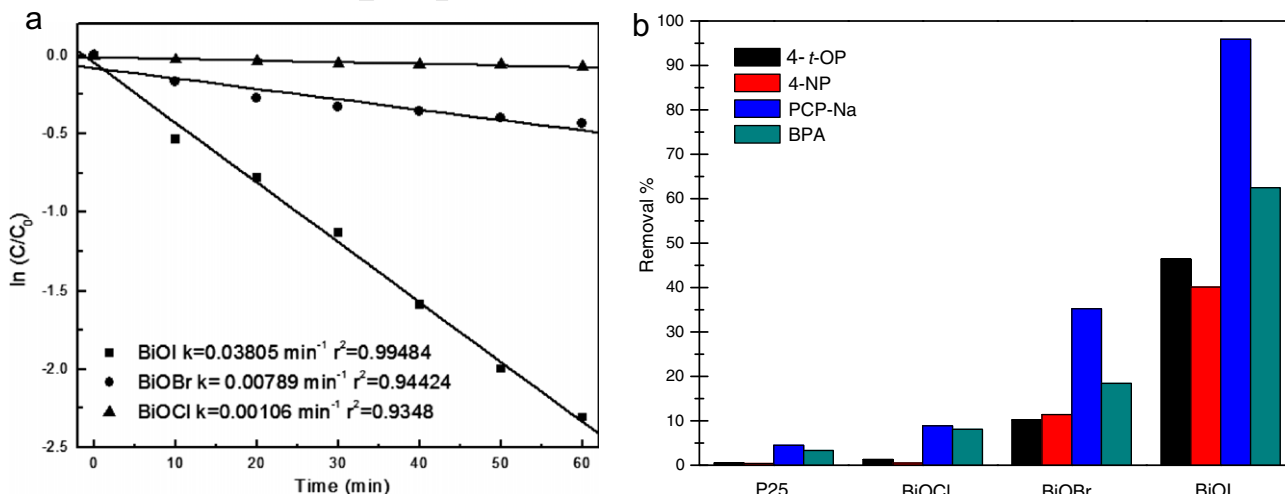


Fig. 3. Photocatalytic activity of organic compounds under Xenon-lamp irradiation: (a) First-order plots for the photocatalytic degradation of PCP-Na over BiOX photocatalysts. (b) Degradation performance towards phenolic EDCs after 2 h photocatalytic process over BiOX and P25.

231 implied that BiOI photocatalyst exhibits the best activity under Xe-
232 non-light irradiation towards four kinds of typical phenolic EDCs
233 because of its narrow band gap.

234 Acknowledgments

235 We acknowledge the financial support in this work by the Na-
236 tional Natural Science Foundation of China (No. 50538090), Na-
237 tional Science Fund for Distinguished Young Scholars of China
238 (No. 50625823), National Key Project of Scientific and Technical
239 Supporting Programs (No. 2007BAC03A09) and Program of “Re-
240 search on Key Technology of Environmental Pollution Control
241 and Quality Improvement (No. 2007DFC90170).”

242 Appendix A. Supplementary data

243 Supplementary data associated with this article can be found, in
244 the online version, at doi:10.1016/j.catcom.2009.11.023.

245 References

246 [1] W. Choi, S.J. Hong, Y.-S. Chang, Y. Cho, Environ. Sci. Technol. 34 (2000) 4810–
247 4815.

- [2] K. Zhang, C. Liu, F. Huang, C. Zheng, W. Wang, Appl. Catal. B: Environ. 68 (2006) 248
125–129. 249
- [3] W. Wang, F. Huang, X. Lin, Scri. Mater. 56 (2007) 669–672. 250
- [4] W. Wang, F. Huang, X. Lin, J. Yang, Catal. Commun. 9 (2008) 8–12. 251
- [5] C. Wang, C. Shao, Y. Liu, L. Zhang, Scri. Mater. 59 (2008) 332–335. 252
- [6] H. An, Y. Du, T. Wang, C. Wang, W. Hao, J. Zhang, Rare Metals 27 (2008) 243– 253
250. 254
- [7] X. Zhang, Z. Ai, F. Jia, L. Zhang, J. Phys. Chem. C 112 (2008) 747–753. 255
- [8] W.E. Morgan, W.J. Stec, J.R. Vanwazer, Inorg. Chem. 12 (1973) 953–955. 256
- [9] R. Floresca, M. Kurihara, D.S. Watt, A. Demir, J. Org. Chem. 58 (1993) 2196– 257
2200. 258
- [10] A. Hjelm, C.G. Granqvist, J.M. Wills, Phys. Rev. B 54 (1996) 2346–2445. 259
- [11] J. Tang, Z. Zou, J. Ye, J. Phys. Chem. B 107 (2003) 14265–14269. 260
- [12] L.H. Keith, W.A. Telliard, Environ. Sci. Technol. 13 (1979) 416–423. 261
- [13] G. Mosconi, O. Carnevali, M.F. Franzoni, E. Cottone, I. Lutz, W. Kloas, K. 262
Yamamoto, S. Kikuyama, A.M. Polzonetti-Magni, Gen. Comp. Endocrinol. 126 263
(2002) 125–129. 264
- [14] X. Chang, G. Ji, Q. Sui, J. Huang, G. Yu, J. Hazard. Mater. 166 (2009) 728–733. 265
- [15] X. Chang et al., Photocatalytic decomposition of 4-*t*-octylphenol over NaBiO₃ 266
driven by visible light: Catalytic kinetics and corrosion products 267
characterization, J. Hazard. Mater. (2009), doi:10.1016/j.jhazmat.2009.08.148. 268
- [16] M. Long, W. Cai, J. Cai, B. Zhou, X. Chai, Y. Wu, J. Phys. Chem. B 110 (2006) 269
20211–20216. 270
- [17] W.L. Huang, Q. Zhu, Comput. Mater. Sci. 43 (2008) 1101–1108. 271
272